Heme Protein Dynamics Revealed by Geminate Nitric Oxide Recombination in Mutants of Iron and Cobalt Myoglobin†

Yuri Kholodenko,‡ Edward A. Gooding,‡ Yi Dou,§,|| Masao Ikeda-Saito,§ and Robin M. Hochstrasser*,‡

Department of Chemistry, The University of Pennsylvania, Philadelphia, Pennsylvania 19104, and Department of Physiology and Biophysics, Case Western Reserve University, School of Medicine, Cleveland, Ohio 44106-4970

Received December 22, 1998; Revised Manuscript Received March 24, 1999

ABSTRACT: Nitric oxide myoglobin (MbNO) at 300 K was photodissociated with 405 nm pulses. The NO recombination in several mutants of iron and cobalt myoglobins was investigated at a time resolution of ca. 70 fs. The geminate recombination of NO was nonexponential on sub-nanosecond time scales. For both metals, the change of the detailed structure of the heme pocket (position 68 mutations) caused significant changes in the rates of recombination; however, the metal substitution influenced the recombination much less than did amino acid substitution. The results indicate a primary role of the heme pocket structure in the dynamics, and they suggest that proximal protein relaxation is not the limiting factor in the geminate recombination process. Recombination in cobalt derivatives is somewhat more efficient on the sub-nanosecond time scales than in corresponding iron myoglobins, consistent with other results that show a greater intrinsic reactivity toward the NO of cobalt compared with the iron heme. A comparison of results using Soret band excitation with previous Q-state excitation studies demonstrates that the ligand dissociates with a similar kinetic energy in both cases, suggesting fast intramolecular energy redistribution before dissociation.

The functions of hemoglobin (Hb)[1] and myoglobin (Mb) in transporting and storing oxygen require that O_2 diffuse through these proteins, to and from the heme iron binding site. In addition, the electronic structure of the metal is sensitive to the precise positioning of its ligands. Therefore, the binding and escape of ligand is closely connected with the nuclear motions of the protein (*1*). Direct studies of the essential properties of ligands such as O_2, NO, or CO within heme proteins are made possible by the facile photodissociation of the corresponding heme−diatom complexes. The diatom is released on a ca. 100 fs time scale (*2*, *3*), and its geminate rebinding, escape kinetics, and bimolecular rebinding can be studied by various spectroscopic methods over wide time ranges (*4*−*15*).

The geminate recombination of CO following photodissociation of MbCO exhibits nonexponential character even at physiological temperatures (*16*, *17*). However, the nonexponential contribution is small. The pioneering study on the subject (*8*) reported exponential kinetics with a time constant of 180 ns. In contrast, the recombination kinetics of NO and O_2 are substantially nonexponential and are completed by several hundred picoseconds (*6*, *7*, *12*, *15*). In particular for NO, several processes were proposed to contribute to the nonexponential character of the recombination (*12*). The so-called *inhomogeneous model* invokes a distribution of potential barriers to recombination. The possibility of the dissociating diatomic ligand being associated with different intermediate sites in the pocket with certain probabilities is the central feature of the related *multiple-site model*. The *relaxation model* incorporates a potential barrier that evolves as the heme and protein structures relax following photodissociation. The microscopic origin of a distribution of barriers has been suggested to arise at least partly from the detailed structure of the heme pocket into which the ligand is ejected by photolysis. Consequently, investigations of the ligand kinetics in myoglobins from different species (*10*, *15*) or properly designed single point mutants (*13*, *14*, *18*−*22*) that alter the chemical nature of the heme pocket can be helpful in evaluating the inhomogeneous contributions to geminate recombination.

Nonequilibrium relaxation of the distal pocket (distal relaxation) was proposed to account for CO nonexponential recombination (*16*, *17*). Relaxation of the protein coupled to the metal out-of-plane motion (proximal or heme relaxation) has been suggested to induce nonexponentiality of NO recombination (*12*, *22*, *23*). Changes that may occur in the heme electronic and nuclear structure can be evaluated by replacing the heme iron with cobalt. In contrast to iron, the cobalt atom does not significantly shift its location relative to the heme plane after photodissociation of the ligand (*24*); therefore, a mechanism of relaxation related to this type of motion (proximal relaxation) is not expected to be so significant for CoMb.

† This research was supported by NIH Grants GM12592 (to R.M.H.) and GM51588 (to M.I.-S.) using instrumentation developed under NIH Grant RR01348 (to R.M.H.).

* To whom correspondence should be addressed. Phone: (215) 898-8410. Fax: (215) 898-0590. E-mail: hochstra@sas.upenn.edu.

‡ The University of Pennsylvania.

§ Case Western Reserve University.

|| Present address: Department of Biochemistry and Cell Biology, Rice University, Houston, TX 77005-1892.

[1] Abbreviations: Mb, myoglobin; Hb, hemoglobin; MbCO, carbon monoxide myoglobin; MbNO, nitric oxide myoglobin; CoMb, cobalt-substituted myoglobin; A/D, analog-to-digital; Asp, aspartic acid; WT, wild type; V68A, V68F, and V68I, mutant myoglobins with valine 68 replaced with alanine, phenylalanine, and isoleucine, respectively; MD, molecular dynamics; TPP, *meso*-tetraphenylporphyrinate.

10.1021/bi983022v CCC: $18.00
Published on Web 04/15/1999

We report here on the recombination of nitric oxide (NO) in the wild type and mutants of both iron and cobalt sperm whale myoglobin. The time resolution is improved over previous studies of the same set of mutants (*13*, *18*), and the results allow us to comment on the excitation wavelength dependence of the recombination dynamics.

MATERIALS AND METHODS

Materials. The wild-type sperm whale myoglobin recombinant protein with the proper amino acid (Asp) at position 122 has been expressed in *Escherichia coli* as described in ref *25*. The expression system was created on the basis of the sperm whale myoglobin synthetic gene (*26*) and the expression vector of ref *27*. Site-directed mutagenesis were performed by cassette mutagenesis, as two complementary oligonucleotides annealed and ligated into the expression vector at the *Bgl*II and *Hpa*I sites (*25*). The mutations were confirmed by DNA sequencing. The recombinant sperm whale myoglobins were purified as described previously (*28*). The cobalt-substituted myoglobins were prepared using the methods described by Ikeda-Saito et al. (*29*).

Nitric oxide Mb (MbNO) samples were prepared in a specially designed airtight flask which contained a 1 mm optical cell for static and transient absorption measurements. The Mb samples in phosphate buffer (pH 7.6) were deoxygenated by bubbling N_2, anaerobically reduced by an excess of sodium dithionite, and equilibrated under an NO atmosphere. The NO gas (Aldrich) was scrubbed before being used by bubbling through 15 cm of a saturated aqueous solution of NaOH and passing through 15 cm of distilled water. The concentration of the samples was in the range of 200 μM, yielding absorbances of $\sim$1 optical density unit at the pump wavelength. The measurements were performed immediately after the preparation. The integrity of the samples was verified both before and after measurements by UV−vis spectroscopy.

Methods. To separate electronic relaxation and vibrational cooling and discern details of the nonexponential NO recombination dynamics, transient signals with high accuracy and over a large dynamic range are needed (*15*). The laser system that was used here (*30*) permits data acquisition with high detectivity (typically $\sim$0.08 optical density milliunits per 2000 shots) from tens of femtoseconds to a few nanoseconds. The system was based on a self-modelocked titanium sapphire oscillator (*31*), pumped by an Ar^+ ion laser (Coherent Innova 300); a regenerative amplifier, pumped by the second harmonic of a Q-switched YLF laser (Quantronics Model 527); and a stretcher−compressor pair (*32*). The system yielded 70 fs pulses with 300 μJ per pulse at 810 nm and a repetition rate of 1 kHz. A portion of the output was frequency doubled (BBO, type I) to produce pump pulses at 405 nm. The pump pulses were focused in the sample to a spot with a diameter of 250 μm (fwhm). Special care was taken not to overpump the samples. Transient signals were recorded at several excitation levels prior to the actual measurements to determine the optimum conditions. Typical excitation energies that were used in the experiments were in the range of 0.1−0.5 μJ per pulse. The pump intensity was continuously recorded during experiments to correct the transient signals for excitation energy fluctuations.

Probe light was generated by focusing the 810 nm pulses into a 1 mm sapphire window. The probe pulses, obtained from the white light by means of 10 nm band-pass filters, were delayed with respect to the pump pulses by means of a computerized delay line. To maximize transient signals, the measurements were performed at 590 nm for iron proteins and at 577 nm for cobalt proteins (we have verified that recombination dynamics is wavelength-independent). The magnitude of the transient signals in these experiments is considerably smaller than in the visible pump−Soret probe experiments that were reported previously (*12*−*14*, *18*, *22*, *33*).

The geometry of the pump−probe experiment was close to collinear with the angle between the directions of propagation of the two beams being 5°. A chopper was used in the pump arm to reduce the excitation rate to 500 Hz for measurements of the absorbance with and without excitation. Silicon diodes were used to detect probe light. The signals were sent to boxcar amplifiers and digitized in the fast A/D converters for transient absorbance calculation. The relative polarizations of the pump and probe beams were adjusted to 54.7° for magic angle measurements.

The transient absorption dynamics were fitted to a multiexponential model (see the Results). The fitting method is based on Marquardt−Levenberg nonlinear least-squares algorithm (*34*) and includes deconvolution of the instrument function.

RESULTS

The transient dynamics in the wild type (WT) and mutants of MbNO are shown in Figure 1. It is apparent that the dynamics are very different when the residue at position 68 is changed. Complex kinetics are evidenced in all the studied proteins. The least-squares fits to a five-exponential model are also shown in Figure 1. The energy dissipation, including two steps of electronic relaxation ($\tau_1 \approx 100$ fs, $\tau_2 \approx 400$−1000 fs) and vibrational cooling ($\tau_3 \approx 3$−5 ps), is represented by the earlier part of the dynamics and is completed within a few picoseconds (*15*). The subsequent stages of the decay represent NO recombination which is the subject of this paper. The recombination part of the dynamics in all cases can be adequately fitted by a two-exponential decay (time constants τ_4 and τ_5) with an offset (a_∞ in Table 1). This offset represents recombination that is too slow to be measured using the method described here. The fitting parameters are shown in Table 1.

The data in Figure 1 and Table 1 show that for both the isoleucine and phenylalanine mutants as well as for WT proteins, the fraction of the recombined molecules at any given time is somewhat larger in cobalt Mb than in iron Mb. For both metals, the extent of recombination at a given time is the smallest and the largest in the isoleucine and phenylalanine mutants, respectively, with the degree of recombination in WT proteins being intermediate. Both rate constants (Table 1) have respectively larger values for the phenylalanine mutant (both metals) than for the corresponding WT protein. It also follows from a comparison of the corresponding amplitudes that the faster decay component in the V68F mutant represents a larger proportion of the overall decay. The situation is opposite for the isoleucine mutant of both metals; while both time constants have larger values, the role

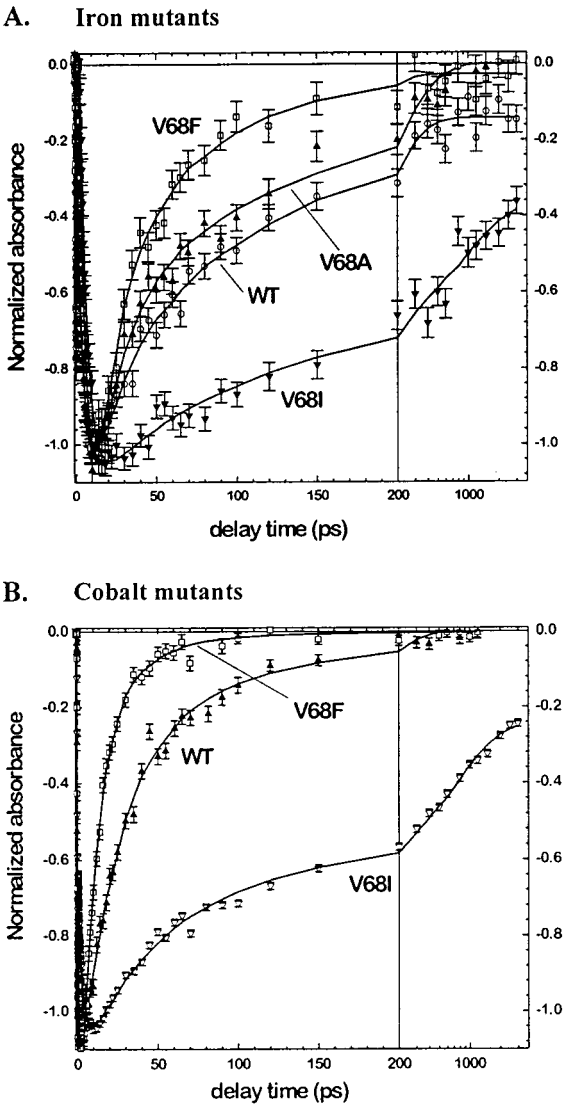

FIGURE 1: Normalized transient absorbance in iron and cobalt mutant MbNO after Soret-state excitation. The actual magnitude of the maximum signals is ca. 2 optical density milliunits. Fits to a multiexponential model are shown (see the text). (A) For iron MbNO, dynamics were probed at 590 nm. (B) For cobalt MbNO, dynamics were probed at 577 nm. The fit parameters are given in Table 1.

of the faster phase is diminished in the V68I mutant compared to that in the WT protein. Furthermore, the longest time component indicated by the offset (a_∞) is quite significant in the isoleucine mutant of both Fe and Co proteins, but in the case of phenylalanine mutants (both metals) or the cobalt WT protein, it has a very small amplitude. Overall, the recombination in the iron V68A mutant is similar to what was found for the WT iron Mb except for the larger offset in WT.

After the energy dissipation processes are completed, the transient absorbance is proportional to the concentration of dissociated molecules $C(t)$. We use this concentration to calculate the instantaneous rate constant of recombination via the equation $k_{rec}(t) = -(dC/dt)/C$. In the frame of the model in which the recombination is represented by a two-exponential decay with an offset, the values of k_{rec} can easily be calculated from the parameters of the fits. The initial rates of recombination (k_{rec} at $t = 0$) for each protein that was studied are also shown in Table 1. They demonstrate the same trends qualitatively seen in the dynamics at later stages. Namely, the initial rates of recombination in cobalt Mb are somewhat higher than in corresponding mutants of iron Mb. For both metals, $k_{rec}(0)$ decreases for the sequence V68F, WT, and V68I. The initial rate of recombination for the iron alanine mutant is only slightly higher than for the iron WT protein.

DISCUSSION

Since the discovery (*7*) that the geminate recombination of NO to the hemes in hemeproteins is a nonexponential process, it has been studied extensively [see a recent review (*35*) for references]. Despite the significant effort, questions remain regarding the microscopic aspects of ligand rebinding in heme proteins. There is no unique experimental demonstration of the cause of the nonexponential behavior of NO recombination. Several mechanisms have been proposed: (i) a distribution of the rebinding rates arising from a static inhomogeneous energy barrier distribution (inhomogeneous model), (ii) different dissociation trajectories of the ligand possibly yielding different intermediate binding sites in the protein each with a different recombination rate (multiple site model), and (iii) a time dependence of the barrier due to protein/heme relaxation toward the unligated structure (relaxation model). The various models cannot be distinguished from fits to the data from kinetic measurements of ligand rebinding.

It is important to relate the details of the protein nuclear structure to the recombination dynamics. High-resolution X-ray structures are available for all deoxy, oxy, CO, and aquomet forms of WT and many mutant myoglobins (*14*, *24*, *36*−*38*). More recently, the high-resolution structure of MbNO was obtained (*39*). Shown in Figure 2 are features of the MbNO structure (*39*) in the vicinity of the heme. Molecular dynamics simulation of MbCO (*40*) and MbNO (*41*) photodissociation shows that the valine at position 68 experiences the largest number of collisions with the ligand after its dissociation. Therefore, it is expected that comparisons of the recombination kinetics for position 68 mutants will provide key information about the role of the heme pocket structure and the associated motions in the dynamics. It should be stressed that the mutations do not significantly affect the overall secondary or tertiary structure of the protein. This was shown by high-resolution X-ray diffraction of the position 68 mutants of sperm whale myoglobin (*14*) which we used in this study. In addition, the relaxation dynamics of the heme iron relative to the heme plane after NO dissociation is not altered upon single point mutations according to MD simulations for position 29 (*21*) and position 68 (*13*) mutants. Thus, it is likely that the changes we observe in the recombination dynamics (Figure 1 and Table 1) are caused by the changes of the structure and dynamics of the distal pocket resulting from single point mutations.

The influence of the out-of-plane metal motion on the recombination dynamics is suggested by a comparison of results for iron- and cobalt-substituted WT and mutant myoglobins. They show that the single point mutations at position 68 influence the course of recombination much more significantly than does the metal substitution (see Figure 3,

Table 1: Parameters for NO Recombination in WT and Mutant Myoglobins[a]

	iron				cobalt		
	Fe, WT	Fe, V68F	Fe, V68I	Fe, V68A	Co, WT	Co, V68F	Co, V68I
τ_4 (ps)	18.9 (41%)	10.1 (78%)	91.4 (35.5%)	20.4 (59%)	24.2 (77%)	10.3 (84%)	48.7 (41%)
τ_5 (ps)	126.4 (49%)	60.2 (21%)	955.8 (32.5%)	182.4 (41%)	117.9 (23%)	33.3 (16%)	727.7 (38%)
a_∞ (%)	10	1	32	0	0	0	21
k_{rec} at $t = 0$ (ns^{-1})	25.8	80.5	4.2	31.1	33.8	86.0	9.0

[a] The transient dynamics were fitted to a five-exponential model with an offset: $\Delta A = \sum_{i=1}^{5} a_i \exp(-t/\tau_i) + a_\infty$. Only the parameters of the recombination part (the last two exponential terms) are shown (see the text for details). Amplitudes have been normalized so that $a_4 + a_5 + a_\infty = 1$. Values of a_4 and a_5 are shown in parentheses.

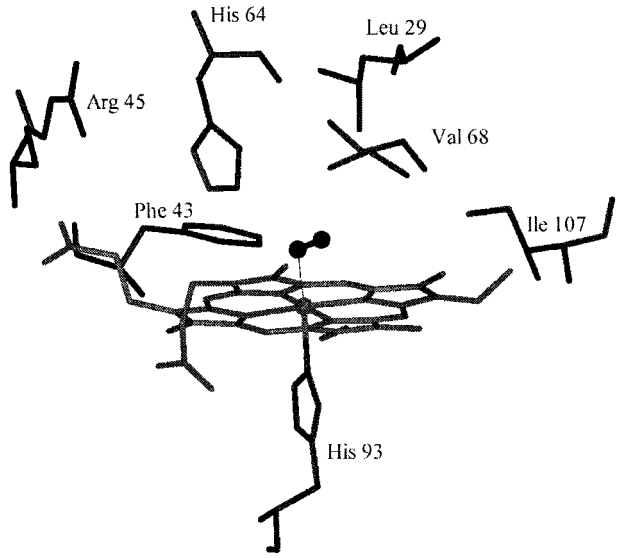

FIGURE 2: Structure in the heme pocket region of WT sperm whale MbNO (Brookhaven Protein Data Bank file name 1HJT) (*39*). Side view of the distal pocket showing the heme, the bound ligand, and several important residues that are discussed in the text.

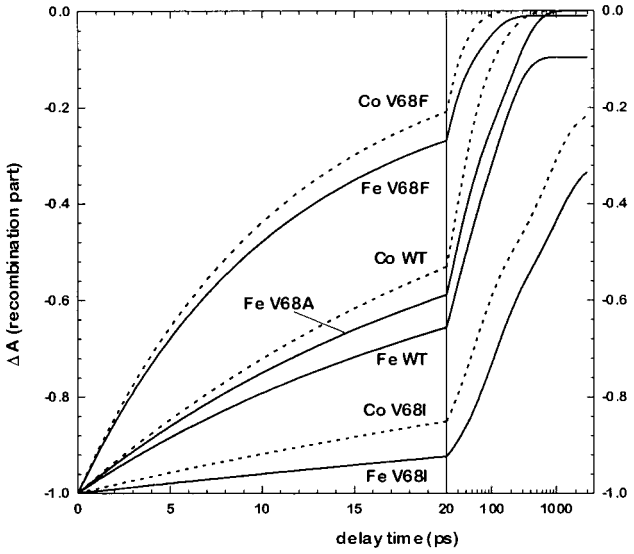

FIGURE 3: NO recombination to iron and cobalt Mb mutants. Only the recombination parts of the fits to the data are shown: iron mutants (—) and cobalt mutants (- - -).

where for clarity only the recombination parts of the fits are shown). The high-resolution crystal structures of cobalt myoglobin derivatives have revealed that the cobalt atom does not undergo as large a displacement as iron from the porphyrin plane when the ligand dissociates (*24*), although the overall structure of cobalt Mb is very similar to the structure of the native iron-containing protein in all the oxy, deoxy, and aquomet forms. One important difference between the structures is the position of the metal with respect to the heme plane. Upon deoxygenation, the iron(II) atom moves 0.16 Å further out of the heme plane, from 0.19 Å in MbO_2 to 0.35 Å in deoxy Mb. The cobalt atom also shows movement out of the porphyrin plane in the same direction, but only by 0.06 Å, from 0.09 Å in the oxy form to 0.15 Å in deoxy. Therefore, in the frame of the proximal relaxation model, the substitution of cobalt for iron should cause changes in the recombination pattern; the recombination of NO in cobalt Mb would be expected to have a less significant inhomogeneous contribution than in the native iron protein. On the other hand, alterations of the heme pocket are not expected to result in significant changes in the proximal relaxation-controlled recombination. The results of our experiments do not exhibit this trend. That is, single mutations at position 68 cause much larger changes in the recombination dynamics than does metal substitution (see Figure 3). Therefore, a proximal relaxation model for nonexponential NO rebinding is not supported by the results, but the importance of the distal pocket in the recombination is evident. Qualitatively, this finding is in agreement with conclusions from previous studies (*13*), where Q-state excitation and slower time resolution were used.

The potential surface for ligand rebinding in Mb should incorporate the changes in spin that occur during the reaction (*7*, *41*−*43*). For the moment neglecting spin−orbit coupling, the recombination in CoMb is a spin-allowed process from a doublet cobalt and doublet ligand to a singlet cobalt−ligand complex (*42*, *43*). Quintet iron and a doublet ligand yield a doublet iron−ligand complex upon recombination in iron Mb (*42*, *43*) in a process requiring a change of one unit of spin angular momentum (*7*, *21*). These spin changes can result in electronic barriers arising from the crossing of potential surfaces (*7*, *44*). This effect was suggested to contribute to the differences in recombination rates for CO, O_2, and NO ligands (*7*). We have found that for both the isoleucine and phenylalanine mutants as well as for WT proteins the fraction of the recombined molecules at any given time is somewhat larger in cobalt Mb than in iron Mb (Figure 3 and Table 1). The reactivities of Fe and Co to NO binding show up in other types of experiments (*45*). The association of NO with the Co^{II} *meso*-tetraphenylporphyrinate complex (Co^{II}TPP) in solution occurs slightly faster than that with Fe^{II}TPP. The bimolecular rate constants in benzene solutions at room temperature were 7.9×10^9 and 5.2×10^9 M^{-1} s^{-1}, respectively (*45*), with both values being slightly lower than expected for a diffusion-limited process (*46*). Moreover, the activation barrier estimated from the temperature depend-

ences of the rate constants in these porphyrin reactions is slightly larger for iron than for cobalt (*47*). These data indicate that the recombination could be kinetically controlled. Our data on NO recombination in iron and cobalt Mb also suggest greater intrinsic reactivity toward NO for cobalt than for the iron porphyrin. This may be a result of there being some spin selectivity remaining, notwithstanding the rather large spin−orbit coupling of iron and cobalt. Proximal energetics effects associated with bringing the metal closer to the heme plane to facilitate ligand binding (*48*) might also contribute to the difference in reactivity in cobalt and iron proteins.

Our data indicate that single point mutations lead to significant changes in the recombination (Figure 3 and Table 1). The extent of recombination at a given time in phenylalanine and isoleucine mutants is much larger and much smaller, respectively, than in the WT protein containing the same metal. The recombination dynamics for the V68A mutant are similar to those for the WT Mb. These results are qualitatively similar to the previous results obtained after Q-state excitation of this set of iron (*13*, *14*, *18*) and cobalt mutants (*13*). An explanation of the difference in recombination between WT and the V68F, V68I, and V68A mutants is suggested by molecular dynamics (MD) simulations (*13*, *14*).

The most recent MD results, based on the structures determined by high-resolution X-ray crystallography (*14*), suggest possible explanations for the difference between bimolecular binding and geminate recombination behavior. There apparently is a water molecule hydrogen-bonded to the N^{ϵ} atom of the distal histidine in the structures of WT, V68A, and V68F deoxy Mb (*14*). The space for this water molecule in the case of the WT and V68A proteins is made available by the small size of the residues at position 68. In the case of V68F, the benzyl side chain points away from the ligand binding site, again leaving enough space for a water molecule. The water molecule restricts bimolecular binding of the ligand to equilibrated deoxy Mb in both the WT and the V68A mutant and may be more important in regulating the Mb function than direct steric interactions between the ligand and heme pocket residues. This results in similar rates of bimolecular binding in these two proteins. The phenylalanine mutant exhibits an unusually low rate of NO bimolecular binding which was explained (*13*, *14*) by a reduction in the speed and extent of ligand movement into the distal pocket due to both the large size of the benzyl side chain and the necessity to expel the water molecule. The X-ray structure of V68I Mb (*14*) shows that the δ methyl group of the isoleucine residue is located close to the metal atom in both deoxy and liganded proteins. In fact, the distal pocket water molecule in the deoxy V68I mutant Mb is displaced by the isoleucine side chain (*14*), so bimolecular ligand binding in the isoleucine mutant does not involve water. The ligand binding is, however, directly hindered by the terminal carbon atom of the isoleucine side chain. The net result is that in the simulation the isoleucine mutant exhibits a rate of bimolecular NO binding which is similar to that in the WT Mb (*13*, *14*) but faster than in the V68F mutant.

Our results for recombination after NO photodissociation from both cobalt and iron proteins do not follow the above predictions for bimolecular kinetics; the degree of recombination in isoleucine mutants is the lowest and in phenylalanine mutants is the highest, with recombination in WT and alanine proteins being intermediate (Figure 3 and Table 1). This difference is presumably because the distal water molecule is not present in the structures of liganded myoglobins (*14*, *39*). Therefore, in contrast to bimolecular binding, the water molecule is not involved in the experiments on light-induced geminate recombination. Molecular dynamics simulations were also used to estimate the number and time distribution of metal−ligand collisions after ligand dissociation from the heme (*14*). The collision dynamics for the V68A mutant are similar to those found in some of the trajectories for the WT protein. In other WT trajectories, the ligand moves quickly to the back of the distal pocket (for details, see Figure 4 in ref *14*). This ligand behavior results in slightly more efficient recombination on the subnanosecond time scales in the alanine mutant compared with the WT Mb (Figure 3 and Table 1). The volume of the distal pocket that is accessible to the ligand in the WT mutant is reduced 2-fold in the phenylalanine mutant by the presence of the bulky benzyl side chain (*14*). The diffusion of the photodissociated ligand away from the metal of the heme is thereby obstructed in the V68F mutant, resulting in a faster geminate recombination (Figure 3 and Table 1). In the V68I mutant, on the other hand, the NO molecules can leave the immediate neighborhood of the iron atom more readily, and the C^{δ} atom of isoleucine 68 can then move across the face of the heme, preventing recombination (*13*, *14*). This mechanism explains both the inefficient recombination and the large amplitude of the offset in the V68I mutant (Figure 3 and Table 1). In addition, in the isoleucine mutant several discrete sites are available to the ligand, only one of which is typically occupied in a given simulation (*14*). This finding is consistent with our experiment; the large proportion of the slow phase in recombination could correspond to the slow return of ligands from sites distant from the iron atom.

Relaxation of the distal pocket has also been proposed to account for nonexponential geminate rebinding of CO (*16*, *17*). In broad terms, the photodissociation is assumed to generate a nonequilibrium distribution of Mb substates which then relax. Distal residue mutation is expected to alter these substates and hence the relaxation they control. In the experiments described here, a microscopic picture of the distal residue dynamics is presented that is not inconsistent with these general features of CO recombination. In any event, the importance of distal effects in controlling geminate NO recombination is evident. This result is in contrast to the strong proximal effects that are seen for MbNO under low-pH conditions where the iron is four-coordinate (*50*).

It is important to understand whether a higher excitation energy (Soret-state pump vs Q-state pump) leads to the release of a ligand with a higher kinetic energy, and therefore results in different ligand dynamics after photodissociation (altering in this way the observed time course of recombination) or whether the excess energy simply leads to hotter reaction products which then undergo vibrational cooling. Comparison of our results following Soret-state excitation with the previous results (*13*, *18*, *22*) indicates that the amount of excess energy initially deposited by the excitation does not affect recombination dynamics significantly for either iron WT Mb or mutant and cobalt myoglobins. This observation suggests that the ligand dissociates with similar

kinetic energies in both cases. Therefore, the additional energy ($E_{Soret} - E_Q$)/hc (6000 cm^{-1}) remains in the reaction products, suggesting that there is a significant fast intramolecular energy redistribution before the dissociation to deoxy heme and NO occurs.

Although we found that recombination dynamics in the WT sperm whale iron Mb (Figure 3 and Table 1) are similar to those found for the WT human Mb (*22*), there is a significant difference between our data and the results reported for the V68A iron mutant of human Mb (*22*). The recombination in the V68A mutant of sperm whale Mb following Soret-state excitation (Figure 3 and Table 1) is significantly slower than recombination in the V68A mutant of human Mb following Q-state excitation (see Figure 2 and Table 1 in ref *22*). There are a number of differences between the primary sequences of human and sperm whale proteins (*51*). Further experiments are needed to identify those sites that are responsible for the evident difference in the recombination dynamics.

SUMMARY

We have shown that changes in the detailed structure of the heme pocket achieved by the single point mutations at position 68 lead to profound changes in the recombination of NO in both iron and cobalt Mb; the amount of recombination at a given time in isoleucine and phenylalanine mutants is much smaller and much larger, respectively, than in the WT protein containing the same metal. This finding supports the results of MD simulations of NO recombination in Mb. Comparison of the recombination in the set of mutants of iron and cobalt Mb shows that the metal substitution influences the course of recombination much less than does amino acid substitution. Therefore, our results are consistent with the primary role of NO diffusion as determined by the details of the distal heme pocket structure and dynamics and thus suggest that the proximal protein relaxation is not the limiting factor in the recombination process.

Recombination in cobalt derivatives is somewhat more efficient on the sub-nanosecond time scales than in corresponding mutants of iron Mb. This finding is consistent with the results from studies on NO binding to metal porphyrins in protein free solutions in which a greater intrinsic reactivity of cobalt than of the iron heme was found.

Qualitatively, our results for NO recombination after Soret band excitation are similar to those where Q-state excitation was used. This suggests that the ligand dissociates with similar kinetic energies in both cases. The excess energy, therefore, mainly influences the reaction product internal states, suggesting fast intramolecular energy redistribution before dissociation.

REFERENCES

1. Case, D. A., and Karplus, M. (1979) *J. Mol. Biol. 132*, 343−368.
2. Martin, J. L., Migus, A., Poyart, C., Lecarpenter, Y., Astier, R., and Antonetti, A. (1983) *Proc. Natl. Acad. Sci. U.S.A. 80*, 173−177.
3. Zhu, L., Zhong, G., Unno, M., Sligar, S. G., and Champion, P. M. (1996) *Biospectroscopy 2*, 301−309.
4. Austin, R. H., Benson, K. W., Eisenstein, L., Frauenfelder, H., and Gunsalus, I. C. (1975) *Biochemistry 14*, 5355−5373.
5. Greene, B. I., Hochstrasser, R. M., Weisman, R. B., and Eaton, W. A. (1978) *Proc. Natl. Acad. Sci. U.S.A. 75*, 5255−5259.
6. Chernoff, D. A., Hochstrasser, R. M., and Steele, A. W. (1980) *Proc. Natl. Acad. Sci. U.S.A. 77*, 5606−5610.
7. Cornelius, P. A., Hochstrasser, R. M., and Steele, A. W. (1983) *J. Mol. Biol. 163*, 119−128.
8. Henry, E. R., Sommer, J. H., Hofrichter, J., and Eaton, W. A. (1983) *J. Mol. Biol. 166*, 443−451.
9. Henry, E. R., Levitt, M., and Eaton, W. A. (1985) *Proc. Natl. Acad. Sci. U.S.A. 82*, 2034−2038.
10. Jongeward, K. A., Masters, J. C., Mitchell, M. J., Magde, D., and Sharma, V. S. (1986) *Biochem. Biophys. Res. Commun. 140*, 962−966.
11. Jongeward, K. A., Magde, D., Taube, D. J., Masters, J. C., Traylor, T. G., and Sharma, V. S. (1988) *J. Am. Chem. Soc. 110*, 380−387.
12. Petrich, J. W., Lambry, J.-C., Kuczera, K., Karplus, M., Poyart, C., and Martin, J.-L. (1991) *Biochemistry 30*, 3975−3987.
13. Ikeda-Saito, M., Dou, Y., Yonetani, T., Olson, J. S., Li, T., Regan, R., and Gibson, Q. H. (1993) *J. Biol. Chem. 268*, 6855−6857.
14. Quillin, M. L., Li, T., Olson, J. S., Phillips, G. N., Jr., Dou, Y., Ikeda-Saito, M., Regan, R., Carlson, M., Gibson, Q. H., Li, H., and Elber, R. (1995) *J. Mol. Biol. 245*, 416−436.
15. Kholodenko, Y., Volk, M., Gooding, E., and Hochstrasser, R. M. (1996) in *Ultrafast Phenomena X* (Barbara, P. F., Fujimoto, J. G., Knox, W. H., and Zinth, W., Eds.) pp 351−352, Springer-Verlag, New York.
16. Lambright, D. G., Balasubramanian, S., and Boxer, S. G. (1993) *Biochemistry 32*, 10116−10124.
17. Tian, W. D., Sage, J. T., Srajer, V., and Champion, P. M. (1992) *Phys. Rev. Lett. 68*, 408−411.
18. Carver, T. E., Rohlfs, R. J., Olson, J. S., Gibson, Q. H., Blackmore, R. S., Springer, B. A., and Sligar, S. G. (1990) *J. Biol. Chem. 265*, 20007−20020.
19. Carver, T. E., Olson, J. S., Smerdon, S. J., Krzywda, S., Wilkinson, A. J., Gibson, Q. H., Blackmore, R. S., Ropp, J. D., and Sligar, S. G. (1991) *Biochemistry 30*, 4697−4705.
20. Gibson, H. Q., Regan, R., Elber, R., Olson, J. S., and Carver, T. E. (1992) *J. Biol. Chem. 267*, 22022−22034.
21. Li, H., Elber, R., and Straub, J. E. (1993) *J. Biol. Chem. 268*, 17908−17916.
22. Petrich, J. W., Lambry, J.-C., Balasubramanian, S., Lambright, D. C., Boxer, S. G., and Martin, J.-L. (1994) *J. Mol. Biol. 238*, 437−444.
23. Kuczera, K., Lambry, J.-C., Martin, J.-L., and Karplus, M. (1993) *Proc. Natl. Acad. Sci. U.S.A. 90*, 5805−5807.
24. Brucker, E. A., Olson, J. S., Phillips, G. N., Jr., Dou, Y., and Ikeda-Saito, M. (1996) *J. Biol. Chem. 271*, 25419−25422.
25. Dou, Y. (1997) Ph.D. Thesis, Case Western Reserve University, Cleveland, OH.
26. Springer, B. A., and Sligar, S. G. (1987) *Proc. Natl. Acad. Sci. U.S.A. 84*, 8961−8965.
27. Nagai, K., and Thogersen, H. C. (1987) *Methods Enzymol. 153*, 461−481.
28. Ikeda-Saito, M., Hori, H., Anderson, L. A., Prince, R. C., Pickering, I. J., George, G. N., Sanders, C. R., Lutz, R. S., McKelvey, E. J., and Mattera, R. (1992) *J. Biol. Chem. 267*, 22843−22852.
29. Ikeda-Saito, M., Lutz, R. S., Shelley, D. A., McKelvey, E. J., Mattera, R., and Hori, H. (1991) *J. Biol. Chem. 266*, 23641−23647.
30. Volk, M., Kholodenko, Y., Lu, H. S. M., Gooding, E. A., DeGrado, W. F., and Hochstrasser, R. M. (1997) *J. Phys. Chem. B 101*, 8607−8616.
31. Asaki, M. T., Huang, C. P., Garvey, D., Zhou, J., Kapteyn, H. C., and Murnane, M. M. (1993) *Opt. Lett. 18*, 977−979.
32. Wynne, K., Reid, G. D., and Hochstrasser, R. M. (1994) *Opt. Lett. 19*, 895−897.
33. Walda, K. N., Liu, X. Y., Sharma, V. S., and Magde, D. (1994) *Biochemistry 33*, 2198−2209.
34. Marquardt, D. W. (1963) *J. Soc. Ind. Appl. Mater. 11*, 431−441.
35. Olson, J. S., and Phillips, G. N., Jr. (1996) *J. Biol. Chem. 271*, 17593−17596.

36. Quilin, M. L., Arduini, R. M., Olson, J. S., and Phillips, G. N., Jr. (1993) *J. Mol. Biol. 234*, 140−155.
37. Phillips, G. N., Jr., Arduini, R. M., Springer, B. A., and Sligar, S. G. (1990) *Proteins: Struct., Funct., Genet. 7*, 358−365.
38. Hubbard, S. R., Hendrickson, W. A., Lambright, D. G., and Boxer, S. G. (1990) *J. Mol. Biol. 213*, 215−218.
39. Brucker, E. A., Olson, J. S., Ikeda-Saito, M., and Phillips, G. N., Jr. (1998) *Proteins: Struct., Funct., Genet. 30*, 352−356.
40. Elber, R., and Karplus, M. (1990) *J. Am. Chem. Soc. 112*, 9161−9175.
41. Schaad, O., Zhou, H. X., Szabo, A., Eaton, W. A., and Henry, E. R. (1993) *Proc. Natl. Acad. Sci. U.S.A. 90*, 9547−9551.
42. Halton, M. P. (1974) *Inorg. Chim. Acta 8*, 131−136.
43. Halton, M. P. (1974) *Inorg. Chim. Acta 8*, 137−142.
44. Frauenfelder, H., and Wolynes, P. G. (1985) *Science 229*, 337−345.
45. Morlino, E. A., and Rodgers, M. A. J. (1996) *J. Am. Chem. Soc. 118*, 11798−11804.
46. Kapinus, E. I., and Kholodenko, Y. V. (1991) *Russ. J. Phys. Chem. 65*, 197−199.
47. Hoshino, M., and Kogure, M. (1989) *J. Phys. Chem. 93*, 5478−5484.
48. Srajer, V., Reinisch, L., and Champion, P. M. (1988) *J. Am. Chem. Soc. 110*, 6656−6670.
49. Makinen, M. W., Houtchens, R. A., and Caughey, W. S. (1979) *Proc. Natl. Acad. Sci. U.S.A. 76*, 6042−6046.
50. Duprat, A. F., Traulor, T. G., Wu, G.-Z., Coletta, M., Sharma, V. S., Walda, K. N., and Magde, D. (1995) *Biochemistry 34*, 2634−2644.
51. Fasman, G. D. (1977) *Handbook of biochemistry and molecular biology*, Vol. 3, Part A, CRC Press, Cleveland, OH.

BI983022V